A Unified Theory of Adaptive Subspace Detection Part II: Numerical Examples

Pia Addabbo, *Senior Member, IEEE*, Danilo Orlando, *Senior Member, IEEE*, Giuseppe Ricci, *Senior Member, IEEE*, and Louis L. Scharf, *Life Fellow, IEEE*

***Abstract*—This paper is devoted to the performance analysis of the detectors proposed in the companion paper (Orlando et al., 2022) where a comprehensive design framework is presented for the adaptive detection of subspace signals. The framework addresses four variations on subspace detection: the subspace may be known or known only by its dimension; consecutive visits to the subspace may be unconstrained or they may be constrained by a prior probability distribution. In this paper, Monte Carlo simulations are used to compare the detectors derived in (Orlando et al., 2022) with estimate-and-plug (EP) approximations of the generalized likelihood ratio (GLR) detectors. Remarkably, some of the EP approximations appear here for the first time (at least to the best of the authors' knowledge). The numerical examples indicate that GLR detectors are effective for the detection of *partially-known signals* affected by inherent uncertainties due to the system or the operating environment. In particular, if the signal subspace is known, GLR detectors tend to ouperform EP detectors. If, instead, the signal subspace is known only by its dimension, the performance of GLR and EP detectors is very similar. Actually, there does not exist a general rule for recommending the first-order approach with respect to the second-order one and vice versa. Nevertheless, the analysis contains a specific case where the second-order detectors can outperform the first-order detectors.**

***Index Terms*—Adaptive detection, alternating optimization, generalized likelihood ratio test, subspace model.**

I. Introduction and Problem Formulation

ADAPTIVE detection of targets modeled as belonging to suitable subspaces has been widely investigated by the signal processing community with applications ranging from radar and sonar to communications and hyperspectral imaging [2], [3], [4], [5], [6], [7], [8], [9], [10], [11]. In the context of radar signal processing, the general framework devised in [12] for homogeneous environments where test and training samples share the same Gaussian distribution has been extended over the years by including unknown scaling differences between test and training samples [13], structured interference components as well as non-Gaussian disturbances [14], [15].

As stated in the companion paper [1], most of these works deal with deterministic targets embedded in random disturbance with unknown covariance matrix. The term deterministic means that target signatures do not obey any prior distribution and, hence, target coordinates within the subspace are not random variables. Generally speaking, this design assumption is referred to as a *first-order (signal) model*. On the contrary in a *second-order (signal) model*, the signal coordinates in the subspace are random variables and parameters of the signal signature appear in second-order statistics such as the covariance matrix. The first application of the second-order model to target detection in partially-homogeneous Gaussian environment can be found in [16], where the estimate-and-plug (EP) approximation to the generalized likelihood ratio test (GLRT) has been used, as in [17]. This approach consists in computing the GLRT assuming that a subset of parameters is known. Then, in order to make the detector fully adaptive, the known parameters are replaced with suitable estimates. The main advantage of the estimate-and-plug approximation is that the resulting detectors have lower computational complexity than their generalized likelihood ratio (GLR) counterparts. But there is generally a loss in performance, and it is this loss that we aim to quantify in this paper.

The second-order model has been further investigated in the companion paper [1], where a unified theoretical framework for subspace adaptive detection (including the first-order model) in Gaussian disturbance has been devised. More importantly, the exact GLRT or suitable approximations of it have been therein derived for the first time (at least to the best of authors' knowledge). These approximations rely on cyclic estimation procedures [18] where, at each step, closed-form updates of the parameter estimates are computed.

Manuscript received 4 April 2022; revised 14 July 2022 and 8 September 2022; accepted 8 September 2022. Date of publication 12 September 2022; date of current version 25 October 2022. The associate editor coordinating the review of this manuscript and approving it for publication was Prof. Yao Xie. The work of Louis L. Scharf was supported in part by the US Office of Naval Research under Grant N00014-21-1-2145 and in part by the US Airforce Office of Scientific Research under Grant FA9550-21-1-0169. *(Corresponding author: Giuseppe Ricci.)*

Pia Addabbo is with the Università degli Studi Giustino Fortunato, 82100 Benevento, Italy (e-mail: p.addabbo@unifortunato.eu).

Danilo Orlando is with the Università degli Studi "Niccolò Cusano", 00166 Roma, Italy (e-mail: danilo.orlando@unicusano.it).

Giuseppe Ricci is with the Dipartimento di Ingegneria dell'Innovazione, Università del Salento, and Consorzio Nazionale Interuniversitario per le Telecomunicazioni, 73100 Lecce, Italy (e-mail: giuseppe.ricci@unisalento.it).

Louis L. Scharf is with the Departments of Mathematics and Statistics, Colorado State University, Fort Collins, CO 80521 USA (e-mail: scharf@colostate.edu).

This article has supplementary downloadable material available at https://doi.org/10.1109/TSP.2022.3206105, provided by the authors.

Digital Object Identifier 10.1109/TSP.2022.3206105

Following the conventions of [1],[1] let us consider a detection system that collects data from a primary and a secondary channel. Data under test are those from the primary channel and are denoted by $\boldsymbol{Z}_P = [\boldsymbol{z}_1 \cdots \boldsymbol{z}_{K_P}] \in \mathbb{C}^{N\times K_P}$, whereas data from the secondary channel, used for the estimation of the disturbance parameters, are indicated by $\boldsymbol{Z}_S = [\boldsymbol{z}_{K_P+1} \cdots \boldsymbol{z}_{K_P+K_S}] \in \mathbb{C}^{N\times K_S}$. In the case of first-order models, the detection problem at hand can be formulated as [1]

$$\begin{cases} H_0: & \begin{cases} \boldsymbol{Z}_P \sim \mathcal{CN}_{NK_P}(\boldsymbol{0}_{N,K_P}, \boldsymbol{I}_{K_P} \otimes \boldsymbol{R}) \\ \boldsymbol{Z}_S \sim \mathcal{CN}_{NK_S}(\boldsymbol{0}_{N,K_S}, \boldsymbol{I}_{K_S} \otimes \gamma\boldsymbol{R}) \end{cases} \\ H_1: & \begin{cases} \boldsymbol{Z}_P \sim \mathcal{CN}_{NK_P}(\boldsymbol{H}\boldsymbol{X}, \boldsymbol{I}_{K_P} \otimes \boldsymbol{R}) \\ \boldsymbol{Z}_S \sim \mathcal{CN}_{NK_S}(\boldsymbol{0}_{N,K_S}, \boldsymbol{I}_{K_S} \otimes \gamma\boldsymbol{R}) \end{cases} \end{cases} \quad (1)$$

where $\boldsymbol{H} \in \mathbb{C}^{N\times r}$ is either a known matrix or an unknown matrix with known rank r, $r \leq N$, $\boldsymbol{X} = [\boldsymbol{x}_1 \cdots \boldsymbol{x}_{K_P}] \in \mathbb{C}^{r\times K_P}$ is the matrix of the unknown signal coordinates, $\boldsymbol{R} \in \mathbb{C}^{N\times N}$ is an unknown positive definite covariance matrix, and $\gamma > 0$ is either a known or an unknown parameter. In the following, we suppose that $K_S \geq N$. Without loss of generality, we assume that $\boldsymbol{H}$ is an arbitrary unitary basis for a subspace that is either known or known only by its dimension.

The hypothesis test based upon the second-order model is formulated as

$$\begin{cases} H_0: & \begin{cases} \boldsymbol{Z}_P \sim \mathcal{CN}_{NK_P}(\boldsymbol{0}_{N,K_P}, \boldsymbol{I}_{K_P} \otimes \boldsymbol{R}) \\ \boldsymbol{Z}_S \sim \mathcal{CN}_{NK_S}(\boldsymbol{0}_{N,K_S}, \boldsymbol{I}_{K_S} \otimes \gamma\boldsymbol{R}) \end{cases} \\ H_1: & \begin{cases} \boldsymbol{Z}_P \sim \mathcal{CN}_{NK_P}(\boldsymbol{0}_{N,K_P}, \boldsymbol{I}_{K_P} \otimes (\boldsymbol{H}\boldsymbol{R}_{xx}\boldsymbol{H}^\dagger + \boldsymbol{R})) \\ \boldsymbol{Z}_S \sim \mathcal{CN}_{NK_S}(\boldsymbol{0}_{N,K_S}, \boldsymbol{I}_{K_S} \otimes \gamma\boldsymbol{R}) \end{cases} \end{cases} \quad (2)$$

where $\boldsymbol{R}_{xx} \in \mathbb{C}^{r\times r}$ is an unknown positive semidefinite matrix (in order to account for possible correlated sources [19, and references therein]). It is important to observe that when the scaling factor γ is known, both (1) and (2) account for a homogeneous environment where primary and secondary data share the same statistical characterization of the disturbance. In fact, secondary data can be equalized, so it is as if $\gamma = 1$. On the other hand, when γ is unknown, the corresponding operating scenario is referred to as partially-homogeneous [13]. The latter model is an extension of the homogeneous environment and, though preserving a relative mathematical tractability, it leads to an increased robustness to inhomogeneities since the assumed difference in power level accounts for terrain type variations, height profile, and shadowing which may appear in practice [20].

In this paper, we assess the performance of the GLR detectors derived in the first part [1] by analyzing probability of detection and false alarm rate. In addition, we compare these performance metrics with those returned by the estimate-and-plug approximations (that are derived in the next subsections). Even though these competitors can be obtained by exploiting existing derivations [2], [16], [21], some of them appear here for the first time.

The remainder of this paper is organized as follows. In the next section, the detection architectures derived in the first part [1] are summarized and the expressions of the estimate-and-plug competitors are given (their derivations can be found in the attached supplemental material). In Section III, the performance of the GLR and EP detectors are investigated and discussed through numerical examples. Section IV contains concluding remarks and future research tracks.

II. Detection Architectures

The aim of this section is twofold. First, in order to make this second part self-contained, we briefly summarize the decision schemes developed in the companion paper. Second, we provide the expressions of the competitors that are based upon the estimate-and-plug paradigm [17], [22]. Recall that this approach consists in computing the GLRT under the assumption that some parameters are known and in replacing them with suitable estimates. For the case at hand, the covariance matrix of the disturbance is initially supposed known and in the final decision statistic it is replaced by the sample covariance matrix (SCM) computed from secondary data only.

A. GLRT-Based Detectors Summary

The detectors described in this subsection are those derived in the first part of this work [1]. Throughout, the log-likelihood function under H_i is denoted by $L_i(\cdot)$, $i = 0, 1$.

1) First-Order Models: Consider problem (1). The related four cases are listed below.[2]

- **Known subspace $\langle\boldsymbol{H}\rangle$, known** γ: The GLRT for problem (1) with $\gamma = 1$ is referred to as a first-order detector for a signal in a known subspace in a homogeneous environment (FO-KS-HE) and is given by

$$\frac{\det\left[\boldsymbol{I}_{K_P} + \boldsymbol{Z}_P^\dagger \boldsymbol{S}_S^{-1} \boldsymbol{Z}_P\right]}{\det\left[\boldsymbol{I}_{K_P} + \left(\boldsymbol{S}_S^{-1/2}\boldsymbol{Z}_P\right)^\dagger \boldsymbol{P}_G^\perp \left(\boldsymbol{S}_S^{-1/2}\boldsymbol{Z}_P\right)\right]} \underset{H_0}{\overset{H_1}{\gtrless}} \eta \quad (3)$$

  where $\boldsymbol{S}_S = \boldsymbol{Z}_S\boldsymbol{Z}_S^\dagger$ and $\boldsymbol{P}_G^\perp = \boldsymbol{I}_N - \boldsymbol{P}_G$ with $\boldsymbol{P}_G = \boldsymbol{G}(\boldsymbol{G}^\dagger\boldsymbol{G})^{-1}\boldsymbol{G}^\dagger$ and $\boldsymbol{G} = \boldsymbol{S}_S^{-1/2}\boldsymbol{H}$.
- **Known subspace $\langle\boldsymbol{H}\rangle$, unknown** γ: Under the assumption $r < N$ and $\min(K_P, N-r) > \frac{NK_P}{K}$, the GLRT for problem (1) with $\gamma > 0$ is referred to as a first-order

[1] *Notation:* in the sequel, vectors and matrices are denoted by boldface lower-case and upper-case letters, respectively. Symbols $\det(\cdot)$, $\mathrm{Tr}\,(\cdot)$, $(\cdot)^T$, and $(\cdot)^\dagger$ denote the determinant, trace, transpose, and conjugate transpose, respectively. As to numerical sets, $\mathbb{C}$ is the set of complex numbers, $\mathbb{C}^{N\times M}$ is the Euclidean space of $(N\times M)$-dimensional complex matrices, and $\mathbb{C}^N$ is the Euclidean space of N-dimensional complex vectors. $\boldsymbol{I}_n$ and $\boldsymbol{0}_{m,n}$ stand for the $n\times n$ identity matrix and the $m\times n$ null matrix. $\langle\boldsymbol{H}\rangle$ denotes the space spanned by the columns of the matrix $\boldsymbol{H} \in \mathbb{C}^{N\times M}$. Given $a_1,\ldots,a_N \in \mathbb{C}$, $\mathrm{diag}\,(a_1,\ldots,a_N) \in \mathbb{C}^{N\times N}$ indicates the diagonal matrix whose ith diagonal element is a_i. We write $\boldsymbol{z} \sim \mathcal{CN}_N(\boldsymbol{x},\boldsymbol{\Sigma})$ to say that the N-dimensional random vector $\boldsymbol{z}$ is a complex normal random vector with mean vector $\boldsymbol{x}$ and covariance matrix $\boldsymbol{\Sigma}$. Moreover, $\boldsymbol{Z} = [\boldsymbol{z}_1\cdots\boldsymbol{z}_K] \sim \mathcal{CN}_{NK}(\boldsymbol{X}, \boldsymbol{I}_K\otimes\boldsymbol{\Sigma})$, with $\otimes$ denoting Kronecker product and $\boldsymbol{X} = [\boldsymbol{x}_1\cdots\boldsymbol{x}_K]$, means that $\boldsymbol{z}_k \sim \mathcal{CN}_N(\boldsymbol{x}_k,\boldsymbol{\Sigma})$ and the columns of $\boldsymbol{Z}$ are statistically independent. The acronym PDF stands for probability density function. $\widehat{\boldsymbol{R}}_i$ and $\widehat{\gamma}_i$ will denote the (possibly approximated) maximum likelihood (ML) estimates of $\boldsymbol{R}$ and γ, respectively, under the H_i hypothesis, $i = 0, 1$.

[2] As in the companion paper [1], the generic detection threshold will be indicated by η.

detector for a signal in a known subspace in a partially-homogeneous environment (FO-KS-PHE), and is given by

$$\frac{\widehat{\gamma}_0^{\frac{K_P(K-N)}{K}} \det\left[\frac{1}{\widehat{\gamma}_0}\boldsymbol{I}_{K_P}+\boldsymbol{M}_0\right]}{\widehat{\gamma}_1^{\frac{K_P(K-N)}{K}} \det\left[\frac{1}{\widehat{\gamma}_1}\boldsymbol{I}_{K_P}+\boldsymbol{M}_1\right]} \underset{H_0}{\overset{H_1}{\gtrless}} \eta \tag{4}$$

where $\boldsymbol{M}_0 = \boldsymbol{Z}_P^\dagger \boldsymbol{S}_S^{-1}\boldsymbol{Z}_P$, $\boldsymbol{M}_1 = (\boldsymbol{S}_S^{-1/2}\boldsymbol{Z}_P)^\dagger \boldsymbol{P}_G^\perp(\boldsymbol{S}_S^{-1/2}\boldsymbol{Z}_P)$, and $\widehat{\gamma}_i$, $i=0,1$, can be computed using Theorem 1 of [1].

- **Unknown subspace $\langle \boldsymbol{H}\rangle$, known** γ: In this case, if $\min(N,K_P)\geq r+1$, the GLRT for problem (1) with $\gamma=1$ is referred to as a first-order detector for a signal in an unknown subspace in a homogeneous environment (FO-US-HE), and is given by

$$\prod_{i=N-r+1}^{N}\left(1+\sigma_i^2\right) \underset{H_0}{\overset{H_1}{\gtrless}} \eta \tag{5}$$

where $\sigma_1^2 \leq \ldots \leq \sigma_N^2$ are the eigenvalues of $\boldsymbol{S}_S^{-1/2}\boldsymbol{Z}_P\boldsymbol{Z}_P^\dagger\boldsymbol{S}_S^{-1/2}$. When $\min(N,K_P)<r+1$, the GLRT reduces to

$$\det\left(\boldsymbol{I}_N+\boldsymbol{S}_S^{-1/2}\boldsymbol{Z}_P\boldsymbol{Z}_P^\dagger\boldsymbol{S}_S^{-1/2}\right) \underset{H_0}{\overset{H_1}{\gtrless}} \eta. \tag{6}$$

- **Unknown subspace $\langle \boldsymbol{H}\rangle$, unknown** γ: Under the conditions $\min(N,K_P)\geq r+1$ and $\min(N,K_P) > NK_P/K+r$, the GLRT for problem (1) is referred to as a first-order detector for a signal in an unknown subspace in a partially-homogeneous environment (FO-US-PHE), and is given by

$$\frac{\widehat{\gamma}_0^{N\left(1-\frac{K_P}{K}\right)}\prod_{i=1}^{N}\left(\frac{1}{\widehat{\gamma}_0}+\sigma_i^2\right)}{\widehat{\gamma}_1^{N\left(1-\frac{K_P}{K}\right)-r}\prod_{i=1}^{N-r}\left(\frac{1}{\widehat{\gamma}_1}+\sigma_i^2\right)} \underset{H_0}{\overset{H_1}{\gtrless}} \eta \tag{7}$$

where $\widehat{\gamma}_0$ and $\widehat{\gamma}_1$ are computed using Corollary 2 and 1 of [1], respectively.

2) Second-Order Models: For problem (2), the expressions of the related decision rules are summarized below.

- **Known subspace $\langle \boldsymbol{H}\rangle$, known** γ: The approximate GLRT for problem (2) is referred to as a second-order detector for a signal in a known subspace in a homogeneous environment (SO-KS-HE), and is given by

$$L_1(\widehat{\boldsymbol{R}}_1,\widehat{\boldsymbol{R}}_{xx},\boldsymbol{H},1;\boldsymbol{Z}) - L_0(\widehat{\boldsymbol{R}}_0,1;\boldsymbol{Z}) \underset{H_0}{\overset{H_1}{\gtrless}} \eta \tag{8}$$

where $L_0(\widehat{\boldsymbol{R}}_0,1;\boldsymbol{Z})$ is the logarithm of (5) in [1] with $\gamma=1$, and $L_1(\widehat{\boldsymbol{R}}_1,\widehat{\boldsymbol{R}}_{xx},\boldsymbol{H},1;\boldsymbol{Z})$ is given by the logarithm of (28) in [1], with $\widehat{\boldsymbol{R}}_{xx}$ and $\widehat{\boldsymbol{R}}_1$ obtained by iterating (31) and (32) of [1]; the number of iterations, $n_{\max}$, is computed according to the following convergence criterion: $\Delta L_1 = |L_1(\boldsymbol{R}^{(n)},\boldsymbol{R}_{xx}^{(n)},\boldsymbol{H},1;\boldsymbol{Z}) - L_1(\boldsymbol{R}^{(n-1)};\boldsymbol{R}_{xx}^{(n-1)};\boldsymbol{H},1;\boldsymbol{Z})|/|L_1(\boldsymbol{R}^{(n-1)};\boldsymbol{R}_{xx}^{(n-1)};\boldsymbol{H},1;\boldsymbol{Z})| \leq \epsilon_1$ with $\epsilon_1>0$. This procedure is summarized in Algorithm 1.

- **Known subspace $\langle \boldsymbol{H}\rangle$, unknown** γ: In this case, an approximation of the GLRT for problem (2) is referred to as a second-order detector for a signal in a known subspace in a partially-homogeneous environment (SO-KS-PHE), and is given by

$$L_1(\widehat{\boldsymbol{R}}_1,\widehat{\boldsymbol{R}}_{xx},\boldsymbol{H},\widehat{\gamma}_1;\boldsymbol{Z}) - L_0(\widehat{\boldsymbol{R}}_0,\widehat{\gamma}_0;\boldsymbol{Z}) \underset{H_0}{\overset{H_1}{\gtrless}} \eta \tag{9}$$

where $L_0(\widehat{\boldsymbol{R}}_0,\widehat{\gamma}_0;\boldsymbol{Z})$ is the logarithm of the maximum of (5) in [1] with respect to γ obtained by using Theorem 1 of [1], while $\widehat{\boldsymbol{R}}_1$, $\widehat{\boldsymbol{R}}_{xx}$, and $\widehat{\gamma}_1$ are computed through the alternating estimation procedure exploiting (32) and (31) of [1] in conjunction with Theorem 5 of [1]. The procedure, summarized in Algorithm 2, terminates when $n_{\max}$ iterations have been performed; $n_{\max}$ is selected according to the following condition: $\Delta L_2 = |L_1(\boldsymbol{R}^{(n)},\boldsymbol{R}_{xx}^{(n)},\boldsymbol{H},\gamma^{(n)};\boldsymbol{Z}) - L_1(\boldsymbol{R}^{(n-1)};\boldsymbol{R}_{xx}^{(n-1)};\boldsymbol{H},\gamma^{(n-1)};\boldsymbol{Z})|/|L_1(\boldsymbol{R}^{(n-1)};\boldsymbol{R}_{xx}^{(n-1)};\boldsymbol{H},\gamma^{(n-1)};\boldsymbol{Z})| \leq \epsilon_2$ with $\epsilon_2>0$.

- **Unknown subspace $\langle \boldsymbol{H}\rangle$, known** γ: Let $\tilde{\boldsymbol{R}}_{xx} = \boldsymbol{H}\boldsymbol{R}_{xx}\boldsymbol{H}^\dagger$, then, the GLRT for problem (2) is referred to as a second-order detector for a signal in an unknown subspace in a homogeneous environment (SO-US-HE), and is given by

$$L_1(\widehat{\boldsymbol{R}}_1,\widehat{\tilde{\boldsymbol{R}}}_{xx},1;\boldsymbol{Z}) - L_0(\widehat{\boldsymbol{R}}_0,1;\boldsymbol{Z}) \underset{H_0}{\overset{H_1}{\gtrless}} \eta \tag{10}$$

where $L_0(\widehat{\boldsymbol{R}}_0,1;\boldsymbol{Z})$ is given by the logarithm of (5) in [1] and the expression of $L_1(\widehat{\boldsymbol{R}}_1,\widehat{\tilde{\boldsymbol{R}}}_{xx},1;\boldsymbol{Z})$ is found from exploiting Theorem 3 of [1] with $\gamma=1$.

- **Unknown subspace $\langle \boldsymbol{H}\rangle$, unknown** γ: The GLRT for problem (2) is referred to as a second-order detector for a signal in an unknown subspace in a partially-homogeneous environment (SO-US-PHE), and is given by

$$L_1(\widehat{\boldsymbol{R}}_1,\widehat{\tilde{\boldsymbol{R}}}_{xx},\widehat{\gamma}_1;\boldsymbol{Z}) - L_0(\widehat{\boldsymbol{R}}_0,\widehat{\gamma}_0;\boldsymbol{Z}) \underset{H_0}{\overset{H_1}{\gtrless}} \eta \tag{11}$$

where $L_0(\widehat{\boldsymbol{R}},\widehat{\gamma}_0;\boldsymbol{Z})$ is the logarithm of the maximum of (5) in [1] with respect to γ obtained by using Theorem 1 of [1] and $L_1(\widehat{\boldsymbol{R}}_1,\widehat{\tilde{\boldsymbol{R}}}_{xx},\widehat{\gamma}_1;\boldsymbol{Z})$ is computed by jointly exploiting Theorems 3 and 4 of [1].

The steps required to compute the GLRs of all of these detectors are summarized in Algorithms 3–10.

B. Estimate-and-Plug Approximations

Let us recall that the EP detectors presented in what follows are obtained by applying the GLRT under the perfect knowledge of the disturbance covariance matrix and replacing the latter in the final decision statistic with the SCM of the secondary data denoted by $\boldsymbol{S}_{K_S} = (1/K_S)\boldsymbol{Z}_S\boldsymbol{Z}_S^\dagger$. Moreover, without loss of

Algorithm 1: Alternating Procedure for SO-KS-HE.

Input: ϵ_1, $\boldsymbol{\beta}^{(0)}$
Compute: $\widehat{\boldsymbol{R}}_{xx}$, $\widehat{\boldsymbol{R}}_1$
1: Set $n = 0$
2: Estimate $\tilde{\boldsymbol{R}}_{1.2}^{(n+1)}$ and $\boldsymbol{R}_{xx}^{(n+1)}$, given $\boldsymbol{\beta}^{(n)}$ using (31) of [1]
3: Estimate $\boldsymbol{\beta}^{(n+1)}$ given $\tilde{\boldsymbol{R}}_{1.2}^{(n+1)}$ and $\boldsymbol{R}_{xx}^{(n+1)}$ by (32) of [1]
4: Set $n = n + 1$
5: If $n = n_{\max}$ go to step 6 else go to step 2
6: **Output:** $\widehat{\boldsymbol{R}}_{xx}$, $\widehat{\boldsymbol{R}}_1$ computed using $\boldsymbol{\beta}^{(n)}$, $\tilde{\boldsymbol{R}}_{1.2}^{(n)}$ and $\boldsymbol{R}_{xx}^{(n)}$

Algorithm 2: Alternating Procedure for SO-KS-PHE.

Input: ϵ_2, $\boldsymbol{\beta}^{(0)}$
Compute: $\widehat{\boldsymbol{R}}_{xx}$, $\widehat{\boldsymbol{R}}_1$, $\widehat{\gamma}_1$
1: Set $n = 0$
2: Estimate $\tilde{\boldsymbol{R}}_{1.2}^{(n+1)}$, $\boldsymbol{R}_{xx}^{(n+1)}$, and $\gamma^{(n+1)}$, given $\boldsymbol{\beta}^{(n)}$ using (31) and *Theorem 5* of [1]
3: Estimate $\boldsymbol{\beta}^{(n+1)}$ given $\tilde{\boldsymbol{R}}_{1.2}^{(n+1)}$, $\boldsymbol{R}_{xx}^{(n+1)}$, and $\gamma^{(n+1)}$ by (32) of [1]
4: Set $n = n + 1$
5: If $n = n_{\max}$ go to step 6 else go to step 2
6: **Output:** $\widehat{\boldsymbol{R}}_{xx}$, $\widehat{\boldsymbol{R}}_1$, and $\widehat{\gamma}_1$ computed using $\boldsymbol{\beta}^{(n)}$, $\tilde{\boldsymbol{R}}_{1.2}^{(n)}$, $\boldsymbol{R}_{xx}^{(n)}$, and $\gamma^{(n)}$

Algorithm 3: FO-KS-HE.

Input: $\boldsymbol{Z}_P, \boldsymbol{Z}_S, \boldsymbol{H}$
Compute: Decision statistic of FO-KS-HE
1: Compute $\boldsymbol{S}_S^{-1/2} = (\boldsymbol{Z}_S\boldsymbol{Z}_S^\dagger)^{-1/2}$
2: Compute $\boldsymbol{G} = \boldsymbol{S}_S^{-1/2}\boldsymbol{H}$
3: Compute $\boldsymbol{P}_G^\perp = \boldsymbol{I}_N - \boldsymbol{G}(\boldsymbol{G}^\dagger\boldsymbol{G})^{-1}\boldsymbol{G}^\dagger$
4: **Output:** $\frac{\det[\boldsymbol{I}_{K_P}+\boldsymbol{Z}_P^\dagger\boldsymbol{S}_S^{-1}\boldsymbol{Z}_P]}{\det[\boldsymbol{I}_{K_P}+(\boldsymbol{S}_S^{-1/2}\boldsymbol{Z}_P)^\dagger\boldsymbol{P}_G^\perp(\boldsymbol{S}_S^{-1/2}\boldsymbol{Z}_P)]}$

Algorithm 4: FO-KS-PHE.

Input: $\boldsymbol{Z}_P, \boldsymbol{Z}_S, \boldsymbol{H}$
Compute: Decision statistic of FO-KS-PHE
1: If $\min(K_P, N - r) > \frac{NK_P}{K}$ go to step 2 else end
2: Compute $\boldsymbol{S}_S^{-1/2} = (\boldsymbol{Z}_S\boldsymbol{Z}_S^\dagger)^{-1/2}$
3: Compute $\boldsymbol{S}_S^{-1/2}\boldsymbol{Z}_P$
4: Compute $\boldsymbol{M}_0 = \boldsymbol{Z}_P^\dagger\boldsymbol{S}_S^{-1}\boldsymbol{Z}_P$
5: Compute $\widehat{\gamma}_0$, using Theorem 1 of [1]
6: Compute $\boldsymbol{G} = \boldsymbol{S}_S^{-1/2}\boldsymbol{H}$
7: Compute $\boldsymbol{P}_G^\perp = \boldsymbol{I}_N - \boldsymbol{G}(\boldsymbol{G}^\dagger\boldsymbol{G})^{-1}\boldsymbol{G}^\dagger$
8: Compute $\boldsymbol{M}_1 = (\boldsymbol{S}_S^{-1/2}\boldsymbol{Z}_P)^\dagger\boldsymbol{P}_G^\perp(\boldsymbol{S}_S^{-1/2}\boldsymbol{Z}_P)$
9: Compute $\widehat{\gamma}_1$, using Theorem 1 of [1]
10: **Output:** $\frac{\widehat{\gamma}_0^{\frac{K_P(K-N)}{K}}\det\left[\frac{1}{\widehat{\gamma}_0}\boldsymbol{I}_{K_P}+\boldsymbol{M}_0\right]}{\widehat{\gamma}_1^{\frac{K_P(K-N)}{K}}\det\left[\frac{1}{\widehat{\gamma}_1}\boldsymbol{I}_{K_P}+\boldsymbol{M}_1\right]}$

Algorithm 5: FO-US-HE.

Input: $\boldsymbol{Z}_P, \boldsymbol{Z}_S, r$
Compute: Decision statistic of FO-US-HE
1: Compute $\boldsymbol{S}_S^{-1/2} = (\boldsymbol{Z}_S\boldsymbol{Z}_S^\dagger)^{-1/2}$
2: Compute $\boldsymbol{T}_P = \boldsymbol{S}_S^{-1/2}\boldsymbol{Z}_P\boldsymbol{Z}_P^\dagger\boldsymbol{S}_S^{-1/2}$
3: Compute the eigenvalues $\sigma_1^2 \leq \ldots \leq \sigma_N^2$ of $\boldsymbol{T}_P$
4: If $\min(N, K_P) > r + 1$ go to step 5 else go to step 6
5: **Output:** $\prod_{i=N-r+1}^{N}(1+\sigma_i^2)$
6: **Output:** $\det(\boldsymbol{I}_N + \boldsymbol{S}_S^{-1/2}\boldsymbol{Z}_P\boldsymbol{Z}_P^\dagger\boldsymbol{S}_S^{-1/2})$

Algorithm 6: FO-US-PHE.

Input: $\boldsymbol{Z}_P, \boldsymbol{Z}_S, r$
Compute: Decision statistic of FO-US-PHE
1: If $\min(K_P, N) \geq r + 1$ and $\min(K_P, N) > \frac{NK_P}{K} + r$ go to step 2 else end
2: Compute $\boldsymbol{S}_S^{-1/2} = (\boldsymbol{Z}_S\boldsymbol{Z}_S^\dagger)^{-1/2}$
3: Compute $\boldsymbol{T}_P = \boldsymbol{S}_S^{-1/2}\boldsymbol{Z}_P\boldsymbol{Z}_P^\dagger\boldsymbol{S}_S^{-1/2}$
4: Compute the eigenvalues $\sigma_1^2 \leq \ldots \leq \sigma_N^2$ of $\boldsymbol{T}_P$
5: Compute $\widehat{\gamma}_0$ using Corollary 2 of [1]
6: Compute $\widehat{\gamma}_1$ using Corollary 1 of [1]
7: **Output:** $\frac{\widehat{\gamma}_0^{N\left(1-\frac{K_P}{K}\right)}\prod_{i=1}^{N}\left(\frac{1}{\widehat{\gamma}_0}+\sigma_i^2\right)}{\widehat{\gamma}_1^{N\left(1-\frac{K_P}{K}\right)-r}\prod_{i=1}^{N-r}\left(\frac{1}{\widehat{\gamma}_1}+\sigma_i^2\right)}$

Algorithm 7: SO-KS-HE.

Input: $\boldsymbol{Z}_P, \boldsymbol{Z}_S, \boldsymbol{H}$
Compute: Decision statistic of SO-KS-HE
1: Compute $L_0(\widehat{\boldsymbol{R}}_0, 1; \boldsymbol{Z})$ as the logarithm of (5), with $\gamma = 1$, in [1]
2: Compute $\widehat{\boldsymbol{R}}_{xx}$ and $\widehat{\boldsymbol{R}}_1$ using Algorithm 1
3: Compute $L_1(\widehat{\boldsymbol{R}}_1, \widehat{\boldsymbol{R}}_{xx}, \boldsymbol{H}, 1; \boldsymbol{Z})$
4: **Output:** $L_1(\widehat{\boldsymbol{R}}_1, \widehat{\boldsymbol{R}}_{xx}, \boldsymbol{H}, 1; \boldsymbol{Z}) - L_0(\widehat{\boldsymbol{R}}_0, 1; \boldsymbol{Z})$

Algorithm 8: SO-KS-PHE.

Input: $\boldsymbol{Z}_P, \boldsymbol{Z}_S, \boldsymbol{H}$
Compute: Decision statistic of SO-KS-PHE
1: Compute $\boldsymbol{S}_S = \boldsymbol{Z}_S\boldsymbol{Z}_S^\dagger$
2: Compute $\boldsymbol{M}_0 = \boldsymbol{Z}_P^\dagger\boldsymbol{S}_S^{-1}\boldsymbol{Z}_P$
3: Compute $\widehat{\gamma}_0$, using Theorem 1 of [1]
4: Compute $L_0(\widehat{\boldsymbol{R}}_0, \widehat{\gamma}_0; \boldsymbol{Z})$ using the logarithm of (5) in [1]
5: Compute $\widehat{\gamma}_1$, $\widehat{\boldsymbol{R}}_{xx}$, and $\widehat{\boldsymbol{R}}_1$ by means of Algorithm 2
6: Compute $L_1(\widehat{\boldsymbol{R}}_1, \widehat{\boldsymbol{R}}_{xx}, \boldsymbol{H}, \widehat{\gamma}_1; \boldsymbol{Z})$
7: **Output:** $L_1(\widehat{\boldsymbol{R}}_1, \widehat{\boldsymbol{R}}_{xx}, \boldsymbol{H}, \widehat{\gamma}_1; \boldsymbol{Z}) - L_0(\widehat{\boldsymbol{R}}_0, \widehat{\gamma}_0; \boldsymbol{Z})$

generality, we resort to a different formulation where the factor γ scales the second-order characterization of the primary data. Otherwise stated, the covariance matrix of primary data is $\gamma\boldsymbol{R}$ whereas that of secondary data is $\boldsymbol{R}$. The reader is referred to the supplemental material for the derivation of the EP detectors.

Algorithm 9: SO-US-HE.

Input: $\boldsymbol{Z}_P, \boldsymbol{Z}_S, r$

Compute: Decision statistic of SO-US-HE

Compute $L_0(\widehat{\boldsymbol{R}}_0, 1; \boldsymbol{Z})$ given by the logarithm of (5) in [1] with $\gamma = 1$

Compute $L_1(\widehat{\boldsymbol{R}}_1, \widehat{\widehat{\boldsymbol{R}}}_{xx}, 1; \boldsymbol{Z})$ exploiting Theorem 3 of [1] with $\gamma = 1$

Output: $L_1(\widehat{\boldsymbol{R}}_1, \widehat{\widehat{\boldsymbol{R}}}_{xx}, 1; \boldsymbol{Z}) - L_0(\widehat{\boldsymbol{R}}_0, 1; \boldsymbol{Z})$

Algorithm 10: SO-US-PHE.

Input: $\boldsymbol{Z}_P, \boldsymbol{Z}_S, r$

Compute: Decision statistic of SO-US-PHE

Compute $\widehat{\gamma}_0$, using Theorem 1 of [1]

Compute $L_0(\widehat{\boldsymbol{R}}_0, \widehat{\gamma}_0; \boldsymbol{Z})$ as the logarithm of (5) in [1]

Compute $L_1(\widehat{\boldsymbol{R}}_1, \widehat{\widehat{\boldsymbol{R}}}_{xx}, \widehat{\gamma}_1; \boldsymbol{Z})$ by jointly exploiting Theorems 3 and 4 of [1]

Output: $L_1(\widehat{\boldsymbol{R}}_1, \widehat{\widehat{\boldsymbol{R}}}_{xx}, \widehat{\gamma}_1; \boldsymbol{Z}) - L_0(\widehat{\boldsymbol{R}}_0, \widehat{\gamma}_0; \boldsymbol{Z})$

1) First-Order Models: The hypothesis test to be solved in this case is given by (1). Thus, exploiting the derivations in [2], [3], [4], it is possible to prove the following results.

- **Known subspace $\langle \boldsymbol{H} \rangle$, known** γ: Assuming $\gamma = 1$, the EP approximation to the GLRT is

$$\mathrm{Tr}\,[\boldsymbol{Z}_P^\dagger \boldsymbol{S}_{K_S}^{-1/2} \boldsymbol{P}_{H_S} \boldsymbol{S}_{K_S}^{-1/2} \boldsymbol{Z}_P] \underset{H_0}{\overset{H_1}{\gtrless}} \eta \tag{12}$$

where $\boldsymbol{P}_{H_S} = \boldsymbol{H}_S (\boldsymbol{H}_S^\dagger \boldsymbol{H}_S)^{-1} \boldsymbol{H}_S^\dagger$ with $\boldsymbol{H}_S = \boldsymbol{S}_{K_S}^{-1/2} \boldsymbol{H}$. This detector will be referred to as the EP approximation to the first-order detector for a signal in a known subspace in a homogeneous environment (EP-FO-KS-HE).

- **Known subspace $\langle \boldsymbol{H} \rangle$, unknown** γ: In this case, the EP approximation to the GLRT is

$$\frac{\mathrm{Tr}\,[\boldsymbol{Z}_P^\dagger \boldsymbol{S}_{K_S}^{-1} \boldsymbol{Z}_P]}{\mathrm{Tr}\,[\boldsymbol{Z}_P^\dagger \boldsymbol{S}_{K_S}^{-1/2} \boldsymbol{P}_{H_S}^{\perp} \boldsymbol{S}_{K_S}^{-1/2} \boldsymbol{Z}_P]} \underset{H_0}{\overset{H_1}{\gtrless}} \eta \tag{13}$$

where $\boldsymbol{P}_{H_S}^{\perp} = \boldsymbol{I}_N - \boldsymbol{P}_{H_S}$. This detector will be referred to as the EP approximation to the first-order detector for a signal in a known subspace in a partially-homogeneous environment (EP-FO-KS-PHE).

- **Unknown subspace $\langle \boldsymbol{H} \rangle$, known** γ: In this case, the EP approximation to the GLRT is

$$\sum_{i=1}^{\min\{r, K_P\}} \sigma_i^2 \underset{H_0}{\overset{H_1}{\gtrless}} \eta \tag{14}$$

where $\sigma_1^2 \geq \ldots \geq \sigma_N^2 \geq 0$ are the eigenvalues of $\boldsymbol{S}_{K_S}^{-1/2} \boldsymbol{Z}_P \boldsymbol{Z}_P^\dagger \boldsymbol{S}_{K_S}^{-1/2}$. This detector will be referred to as the EP approximation to the first-order detector for a signal in an unknown subspace in a homogeneous environment (EP-FO-US-HE).

- **Unknown subspace $\langle \boldsymbol{H} \rangle$, unknown** γ: In this case, the EP approximation to the GLRT is

$$\frac{\sum_{i=1}^{\min\{r, K_P\}} \sigma_i^2}{\mathrm{Tr}\,[\boldsymbol{Z}_P^\dagger \boldsymbol{S}_{K_S}^{-1} \boldsymbol{Z}_P]} \underset{H_0}{\overset{H_1}{\gtrless}} \eta. \tag{15}$$

This detector will be referred to as the EP approximation to the first-order detector for a signal in an unknown subspace in a partially-homogeneous environment (EP-FO-US-PHE).

2) Second-Order Models: The hypothesis test under consideration is now problem (2). As in the previous subsection, we distinguish four cases.

- **Known subspace $\langle \boldsymbol{H} \rangle$, known** γ: Without loss of generality $\gamma = 1$ and the EP approximation to the GLRT is [16], [21]

$$\mathrm{Tr}\,[\boldsymbol{B}] - K_P \sum_{i=1}^{r_B} \log(1 + \widehat{\lambda}_i) - \sum_{i=1}^{r_B} \frac{\gamma_i}{1 + \widehat{\lambda}_i} \underset{H_0}{\overset{H_1}{\gtrless}} \eta \tag{16}$$

where $\boldsymbol{B} = \boldsymbol{L}^{-1} \boldsymbol{G}^\dagger \boldsymbol{S}_{K_S}^{-1/2} \boldsymbol{Z}_P \boldsymbol{Z}_P^\dagger \boldsymbol{S}_{K_S}^{-1/2} \boldsymbol{G} \boldsymbol{L}^{-\dagger} \in \mathbb{C}^{r \times r}$ with rank $r_B \leq \min\{K_P, r\}$, $\boldsymbol{L} \in \mathbb{C}^{r \times r}$ is such that $\boldsymbol{L}\boldsymbol{L}^\dagger = \boldsymbol{G}^\dagger \boldsymbol{G}$, and $\widehat{\lambda}_i = \max(\gamma_i / K_P - 1, 0)$, $i = 1, \ldots, r_B$, with γ_i, $i = 1, \ldots, r_B$, the eigenvalues of $\boldsymbol{B}$; $\mathrm{Tr}\,[\boldsymbol{B}] = \mathrm{Tr}\,[\boldsymbol{Z}_P^\dagger \boldsymbol{S}_{K_S}^{-1/2} \boldsymbol{P}_G \boldsymbol{S}_{K_S}^{-1/2} \boldsymbol{Z}_P] = \mathrm{Tr}\,[\boldsymbol{Z}_P^\dagger \boldsymbol{S}_{K_S}^{-1/2} \boldsymbol{P}_{H_S} \boldsymbol{S}_{K_S}^{-1/2} \boldsymbol{Z}_P]$. This detector will be referred to as the EP approximation to the second-order detector for a signal in a known subspace in a homogeneous environment (EP-SO-KS-HE).

- **Known subspace $\langle \boldsymbol{H} \rangle$, unknown** γ: The EP approximation to the GLR is [16], [21]

$$\begin{aligned} &K_P N \log \mathrm{Tr}\,[\boldsymbol{Z}_P^\dagger \boldsymbol{S}_{K_S}^{-1} \boldsymbol{Z}_P] - K_P N \log \widehat{\gamma} \\ &\quad - \frac{1}{\widehat{\gamma}} \mathrm{Tr}\,\left(\boldsymbol{Z}_P^\dagger \boldsymbol{S}_{K_S}^{-1/2} \boldsymbol{P}_G^{\perp} \boldsymbol{S}_{K_S}^{-1/2} \boldsymbol{Z}_P \right) \\ &\quad - K_P \sum_{i=1}^{r_B} \log(1 + \widehat{\delta}_i) - \sum_{i=1}^{r_B} \frac{\gamma_i / \widehat{\gamma}}{1 + \widehat{\delta}_i} \end{aligned} \tag{17}$$

where $\widehat{\delta}_i = \max(\gamma_i / (K_P \widehat{\gamma}) - 1, 0)$, $i = 1, \ldots, r_B$, and $\widehat{\gamma}$ is the solution of

$$-\frac{K_P N}{\gamma} + \frac{\mathrm{Tr}\,\left(\boldsymbol{Z}_P^\dagger \boldsymbol{S}_{K_S}^{-1/2} \boldsymbol{P}_G^{\perp} \boldsymbol{S}_{K_S}^{-1/2} \boldsymbol{Z}_P \right)}{\gamma^2} + h(\gamma) = 0 \tag{18}$$

with

$$h(\gamma) = \begin{cases} \frac{K_P r_B}{\gamma}, & \text{if } \gamma < \frac{\gamma_{r_B}}{K_P} \\ \frac{K_P (i-1)}{\gamma} + \frac{\sum_{j=i}^{r_B} \gamma_j}{\gamma 2}, & \text{if } \frac{\gamma_i}{K_P} \leq \gamma < \frac{\gamma_{i-1}}{K_P},\ i = 2, \ldots, r_B \\ \frac{\sum_{i=1}^{r_B} \gamma_i}{\gamma^2}, & \text{if } \frac{\gamma_1}{K_P} \leq \gamma \end{cases}. \tag{19}$$

This detector will be referred to as the EP approximation to the second-order detector for a signal in a known subspace in a partially-homogeneous environment (EP-SO-KS-PHE).

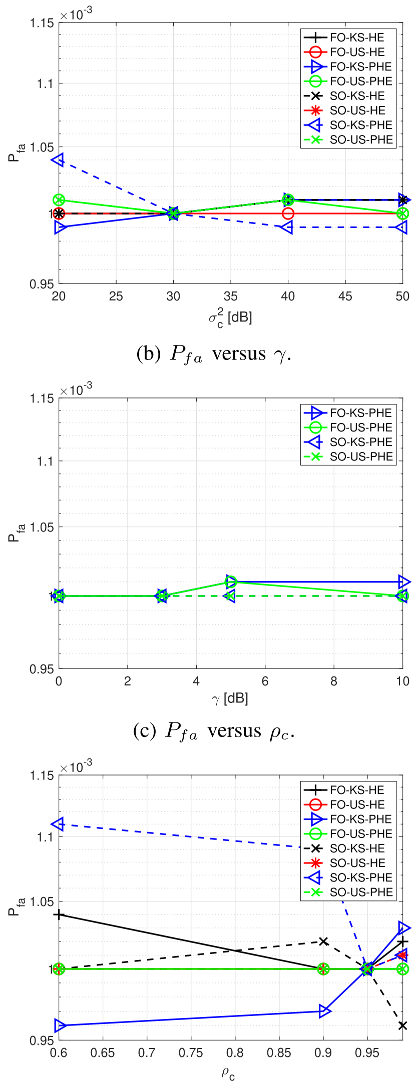

(a) P_{fa} versus σ_c^2.

(b) P_{fa} versus γ.

(c) P_{fa} versus ρ_c.

Fig. 1. Estimated P_{fa} versus σ_c^2 (a), γ (b), and ρ_c (c) for $N = 16$, $K_P = 16$, $K_S = 32$, and $r = 2$. The number of iterations for the alternating procedure is 5. The nominal values of σ_c^2, γ, ρ_c, and P_{fa} are 30 dB, 3 dB, 0.95, and 10^{-3}, respectively.

- **Unknown subspace $\langle \boldsymbol{H} \rangle$, known** γ: Since $\boldsymbol{H}$ is unknown, then $\tilde{\boldsymbol{R}}_{xx} = \boldsymbol{H}\boldsymbol{R}_{xx}\boldsymbol{H}^\dagger$ is an unknown positive semidefinite matrix with rank less than or equal to r. Thus, reasoning in terms of $\tilde{\boldsymbol{R}}_{xx}$ and following the lead of [23], [24], the EP approximation to the GLRT is

$$\mathrm{Tr}[\boldsymbol{Z}_P^\dagger \boldsymbol{S}_{K_S}^{-1} \boldsymbol{Z}_P] - K_P \sum_{i=1}^{r} \log(1+\widehat{q}_i) - \sum_{i=1}^{N} \frac{\sigma_i^2}{1+\widehat{q}_i} \underset{H_0}{\overset{H_1}{\gtrless}} \eta \quad (20)$$

where $\widehat{q}_i = \max(\sigma_i^2/K_P - 1, 0)$, $i = 1, \ldots, r$, $\widehat{q}_i = 0$, $i = r+1, \ldots, N$, and σ_i^2 are sorted in descending order. This detector will be referred to as the EP approximation to the second-order detector for a signal in an unknown subspace in a homogeneous environment (EP-SO-US-HE).

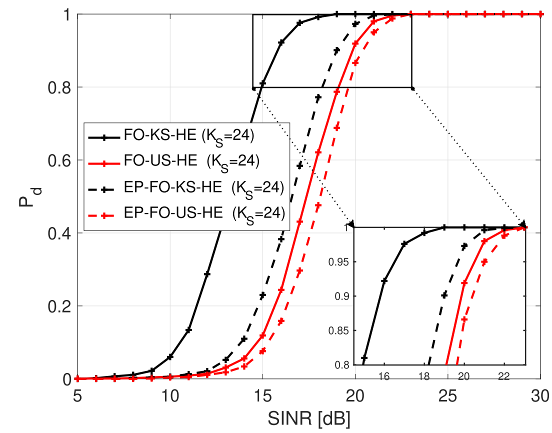

Fig. 2. First-order detectors for homogeneous environment: $N = 16$, $K_P = 16$, $r = 2$, $K_S = 24$, and $P_{fa} = 10^{-3}$.

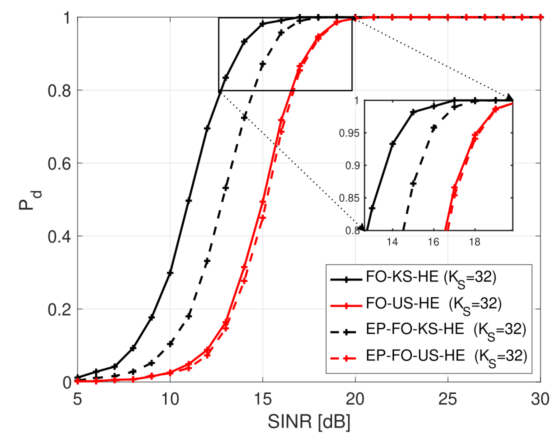

Fig. 3. First-order detectors for homogeneous environment: $N = 16$, $K_P = 16$, $r = 2$, $K_S = 32$, and $P_{fa} = 10^{-3}$.

- **Unknown subspace $\langle \boldsymbol{H} \rangle$, unknown** γ: Denote by $r_0 = \min\{K_P, N\}$ the rank of $\boldsymbol{S}_{K_S}^{-1/2}\boldsymbol{Z}_P\boldsymbol{Z}_P^\dagger\boldsymbol{S}_{K_S}^{-1/2}$ and assume that $r_0 > r$; then, the EP approximation to the GLRT is

$$K_P N \log \mathrm{Tr}\,[\boldsymbol{Z}_P^\dagger \boldsymbol{S}_{K_S}^{-1} \boldsymbol{Z}_P] - K_P \sum_{i=1}^{r} \log(\widehat{\gamma} + \widehat{q}_i) - K_P \sum_{i=r+1}^{N} \log \widehat{\gamma} - \sum_{i=1}^{r} \frac{\sigma_i^2}{\widehat{\gamma}+\widehat{q}_i} - \sum_{i=r+1}^{r_0} \frac{\sigma_i^2}{\widehat{\gamma}} \underset{H_0}{\overset{H_1}{\gtrless}} \eta \quad (21)$$

where $\widehat{q}_i = \max(\sigma_i^2/K_P - \widehat{\gamma}, 0)$, $i = 1, \ldots, r$, and $\widehat{\gamma}$ is the solution of the equation

$$\begin{cases} -\frac{K_P(N-r)}{\gamma} + \frac{\sum_{i=r+1}^{r_0}\sigma_i^2}{\gamma^2} = 0, \text{ if } \frac{\sigma_r^2}{K_P} > \gamma \\ -\frac{K_P(N-i+1)}{\gamma} + \frac{\sum_{j=i}^{r_0}\sigma_j^2}{\gamma^2} = 0, \text{ if } \underset{i=2,\ldots,r}{\frac{\sigma_i^2}{K_P} \le \gamma < \frac{\sigma_{i-1}^2}{K_P}} \\ -\frac{K_P N}{\gamma} + \frac{\sum_{i=1}^{r_0}\sigma_i^2}{\gamma^2} = 0, \text{ if } \frac{\sigma_1^2}{K_P} \le \gamma \end{cases} \quad (22)$$

The detector will be referred to as the EP approximation to the second-order detector for a signal in an unknown

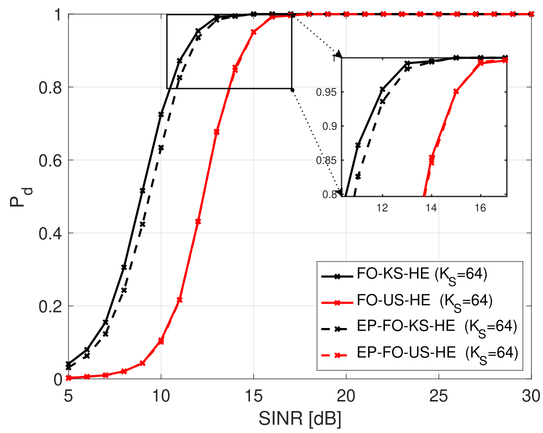

Fig. 4. First-order detectors for homogeneous environment: $N = 16, K_P = 16, r = 2, K_S = 64$, and $P_{fa} = 10^{-3}$.

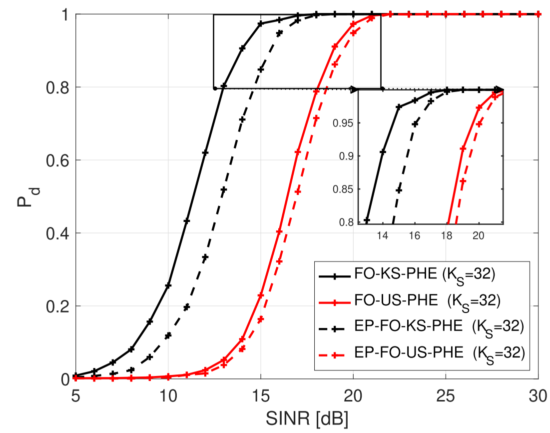

Fig. 6. First-order detectors for partially-homogeneous environment: $N = 16, K_P = 16, r = 2, K_S = 32$, and $P_{fa} = 10^{-3}$.

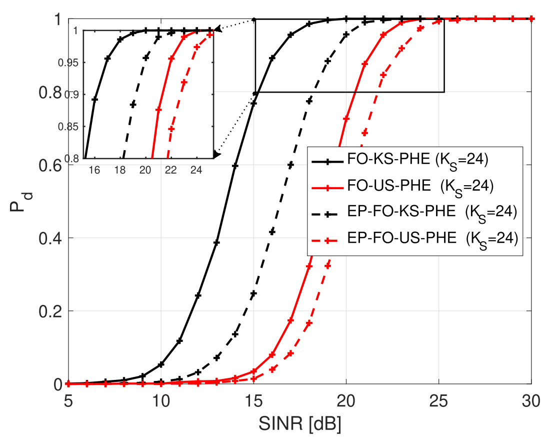

Fig. 5. First-order detectors for partially-homogeneous environment: $N = 16, K_P = 16, r = 2, K_S = 24$, and $P_{fa} = 10^{-3}$.

subspace in a partially-homogeneous environment (EP-SO-US-PHE).

III. Illustrative Examples and Discussion

In this section, Monte Carlo (MC) counting techniques are used to evaluate the performances of the GLR detectors derived in [1], and these are compared to the performances of their EP approximations.

The probability of detection (P_d) and the thresholds to guarantee a given probability of false alarm (P_{fa}) are estimated over 10^3 and $100/P_{fa}$ independent MC trials, respectively. In all the illustrative examples we assume $N = 16$ and $P_{fa} = 10^{-3}$; values of r, K_P, and K_S vary. The covariance matrix, $\boldsymbol{R}$, is $\boldsymbol{R} = \boldsymbol{I}_N + \sigma_c^2 \boldsymbol{M}_c$, with σ_c^2 accounting for a clutter-to-noise ratio of 30 dB assuming unit noise power. The (i, j)th entry of the clutter component $\boldsymbol{M}_c$ is $\rho_c^{|i-j|}$ with $\rho_c = 0.95$. The value of γ for the partially-homogeneous environment is set to 2 (3 dB).

In the simulated scenario the signal component in the ith vector $\boldsymbol{z}_i$, $i = 1, \ldots, K_P$, is given by $\alpha_i \mathbf{v}(\phi_i)$, with $\mathbf{v}(\phi_i) = \frac{1}{\sqrt{N}}[1 \; e^{j\phi_i} \; \cdots \; e^{j(N-1)\phi_i}]^T$; the electrical angles ϕ_i are independent random variables uniformly distributed on $\Phi = [-\pi\beta, \pi\beta]$, where $\beta = \sin\theta$ and θ equals (unless otherwise stated) $2\pi(2/360)$ radians (corresponding to 2°). The interval Φ is discretized using a step of 0.02 radians. Accordingly, we choose the signal subspace by computing the matrix $\boldsymbol{R}_\beta \in \mathbb{C}^{N\times N}$, whose (m, n)th entry is given by [25]

$$\boldsymbol{R}_\beta(m, n) = \beta \frac{\sin((n-m)\beta\pi)}{(n-m)\beta\pi}.$$

When the signal subspace is known it is chosen to be $< \boldsymbol{U}_r >$ where the matrix $\boldsymbol{U}_r \in \mathbb{C}^{N\times r}$ is composed of the first r columns of $\boldsymbol{U} \in \mathbb{C}^{N\times N}$ that in turn consists of the normalized eigenvectors of $\boldsymbol{R}_\beta$ corresponding to its most significant eigenvalues.

A. First-Order Detectors

In this case, we define $\boldsymbol{V}_P = [\mathbf{v}(\phi_1) \cdots \mathbf{v}(\phi_{K_P})]$ and set the magnitude of $\alpha_i = |\alpha| e^{j\varphi_{\alpha,i}}$ according to the signal-to-interference-plus-noise ratio (SINR) defined as

$$\text{SINR} = |\alpha|^2 \text{Tr}\,(\boldsymbol{V}_P^\dagger \boldsymbol{R}^{-1} \boldsymbol{V}_P). \quad (23)$$

The phases $\varphi_{\alpha,i}$ are independent and uniformly distributed in $[0, 2\pi)$.

The analysis starts by assessing to what extent the detection thresholds are sensitive to the variations of σ_c^2, γ, and ρ_c. The results are shown in Fig. 1, where we plot the estimated P_{fa} over $100/P_{fa}$ MC trials assuming a nominal value of 10^{-3}. These results indicate that P_{fa} for all the derived detectors is relatively invariant to σ_c^2, γ, and ρ_c, at least for the considered parameter settings.

Figs. 2–7 are plots of P_d vs SINR for the first-order GLR detectors and their EP approximations. Figs. 2, 3, and 4 assume a homogeneous environment, whereas Figs. 5, 6, and 7 assume a partially-homogeneous environment. The GLR detectors of [1] are represented by solid lines and the EP approximations are represented by dashed lines. Curves of detectors for a known signal subspace are black and curves of detectors for an unknown subspace are red. A zoom box on high values of P_d demonstrates the gains/losses at $P_d = 0.9$. Inspection of the figures shows that detectors for a known signal subspace outperform detectors for

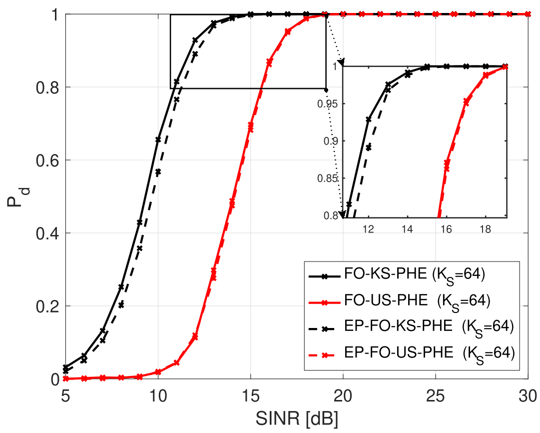

Fig. 7. First-order detectors for partially-homogeneous environment: $N = 16, K_P = 16, r = 2, K_S = 64$, and $P_{fa} = 10^{-3}$.

an unknown subspace, as could be expected. More importantly, GLR detectors for a known signal subspace outperform their EP approximations. The GLR and EP detectors are more or less equivalent under the assumption that the signal subspace is unknown.

To show the influence of K_S on the detection performance, it is possible to compare Figs. 2, 3, and 4 for the homogeneous environment and, similarly, Figs. 5, 6, and 7 for the partially-homogeneous environment. As expected, the better performance obtained for the greater value of K_S for all detectors, with the EP detectors filling the performance gap at $K_S = 64$ due to an enhanced fidelity of the SCM estimate. Additional numerical examples not reported here for brevity confirm this observed behavior for $r = 4$.

B. Second-Order Detectors

Under the second-order model, $\boldsymbol{\alpha} = [\alpha_1 \cdots \alpha_{K_P}]^T$ is a complex Gaussian vector with covariance matrix $\sigma_\alpha^2 \boldsymbol{I}_{K_P}$, with $\sigma_\alpha^2 > 0$ varying according to the SINR defined in (23) with σ_α^2 replacing $|\alpha|^2$. It is important to notice that such a model does not perfectly match the design assumptions of the second-order detectors.

As a preliminary step, we analyze the proposed alternating procedures for iterations h, ranging from 2 to 20. To this end, we plot the average values of $\Delta L_i, i = 1, 2$, over 100 MC trials versus h, in Fig. 8(a)–(d), for both the homogeneous and the partially-homogeneous environments and simulating the null and the alternative hypotheses. All the parameter values used for this analysis are shown in the figures; under H_1 the SINR value is set to 20 dB. It turns out that, for the considered parameters, 5 iterations are sufficient to achieve a relative variation approximately lower than 10^{-5} and this value is also used in what follows.

Figs. 9–14 are plots of P_d vs SINR for the second-order GLR detectors and their EP approximations. Figs. 9, 10, and 11 assume a homogeneous environment while Figs. 12, 13, and 14 assume a partially-homogeneous environment. The GLR

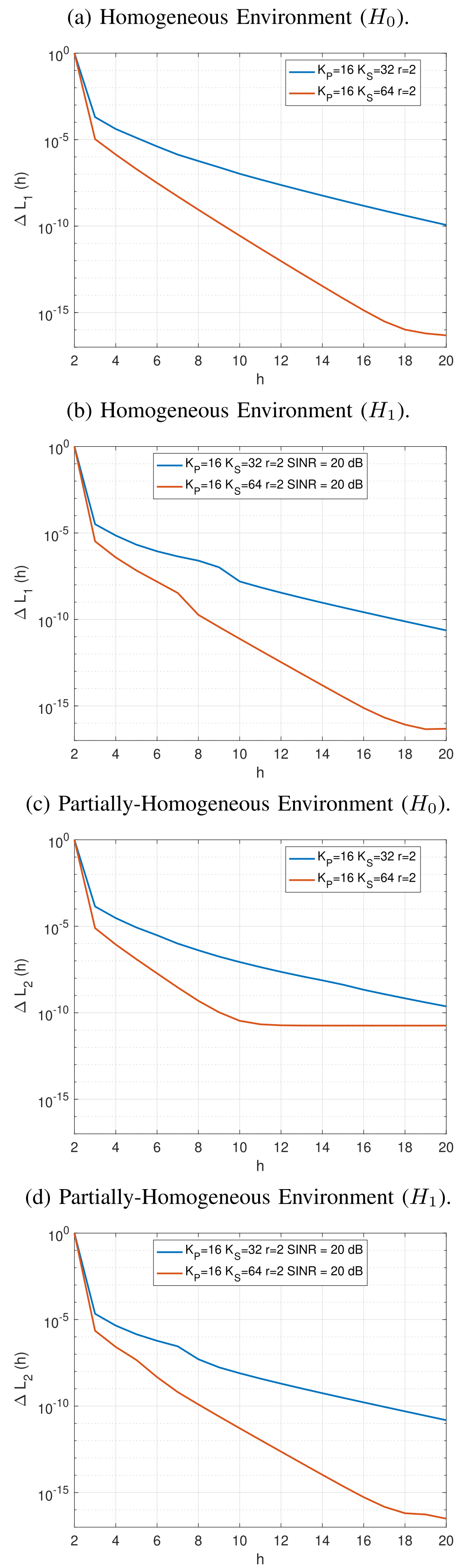

Fig. 8. Log-likelihood variation versus the iteration number of the alternating procedures.

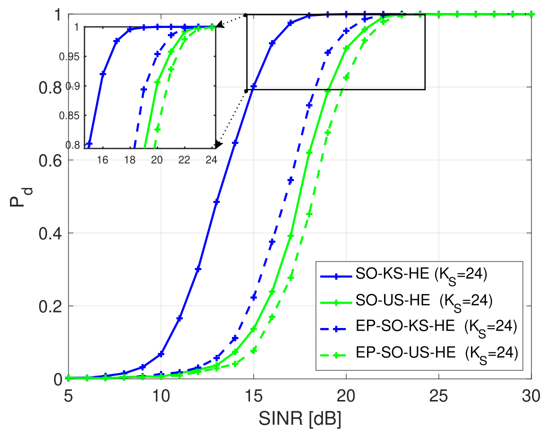

Fig. 9. Second-order detectors for homogeneous environment: $N = 16, K_P = 16, r = 2$, $K_S = 24$, and $P_{fa} = 10^{-3}$.

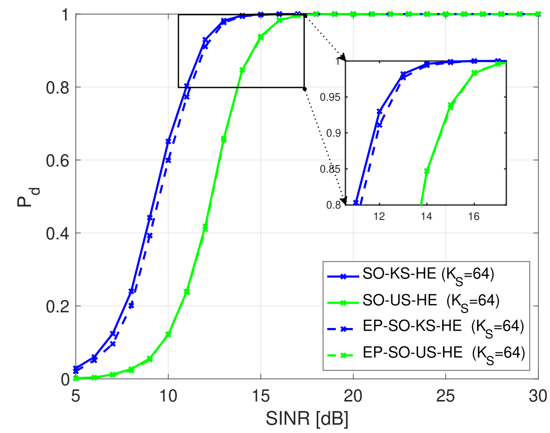

Fig. 11. Second-order detectors for homogeneous environment: $N = 16, K_P = 16, r = 2$, $K_S = 64$, and $P_{fa} = 10^{-3}$.

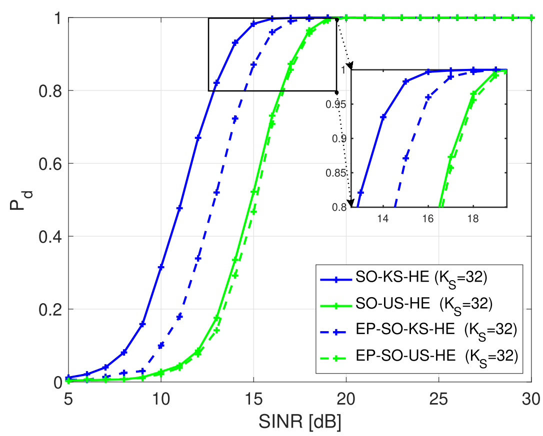

Fig. 10. Second-order detectors for homogeneous environment: $N = 16, K_P = 16, r = 2$, $K_S = 32$, and $P_{fa} = 10^{-3}$.

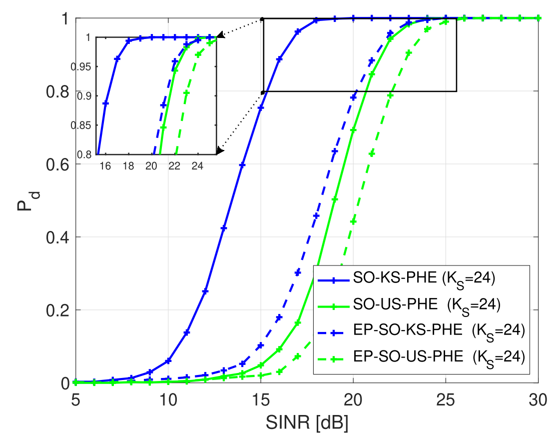

Fig. 12. Second-order detectors for partially-homogeneous environment: $N = 16, K_P = 16, r = 2$, $K_S = 24$, and $P_{fa} = 10^{-3}$.

detectors proposed in [1] are represented by solid lines and the EP approximations are represented by dashed lines. Curves of detectors for a known signal subspace are blue and curves of detectors for an unknown subspace are green. Again a zoom box on high values of P_d is reported. The second-order detectors for a known signal subspace outperform detectors for an unknown signal subspace and GLR detectors for a known signal subspace are better than the corresponding EP detectors for both $K_S = 24$ and $K_S = 32$. However, this time the gain of the GLR detector over the corresponding EP detector is much more pronounced in a partially-homogeneous environment and, in the case of detectors for a known subspace, is still remarkable for $K_S = 64$.

C. Comparison Between First- and Second-Order Detectors

In Figs. 15 and 16, the comparison is conducted by adopting the same parameter values and signal angular sector as in the previous subsections. Moreover, Fig. 15 assumes that the α_ks are deterministic, whereas in Fig. 16 they are Gaussian random variables. The figures highlight that first- and second-order GLR detectors commonly share the same performance.

Nevertheless, the above behavior is no longer true for the scenario associated with Figs. 17 and 18, where a wider angular sector (i.e., θ equals $2\pi(20/360)$ radians leading to $r = 10$) is considered assuming the homogeneous environment and that target coordinates are Gaussian and constant over the range bins of the primary channel. In this case, a gain of the second-order detectors with respect to their first-order counterparts can be observed and the magnitude of such a gain is always larger than 1 dB at least for the considered cases.

For the sake of completeness, we have also compared all the considered detection architectures in terms of the computational time required to return their respective decision statistics.[3] Table I shows the measured execution times for the proposed GLR detectors in comparison with their EP counterparts. It is important to underline that the reported times only refer to the

[3]Notice that we use this computational metric because the usual Landau notation, in the limit of large samples, would lead to similar computational requirements. In fact, all of the considered architectures require the computation and inversion of the sample covariance matrix and it is well known that these operations are $\mathcal{O}(KN^2)$ (recall that we assume $K > N$) and $\mathcal{O}(N^3)$ [26], respectively, representing the most significant terms. However, for finite sample sizes, each algorithm exhibits its own execution time.

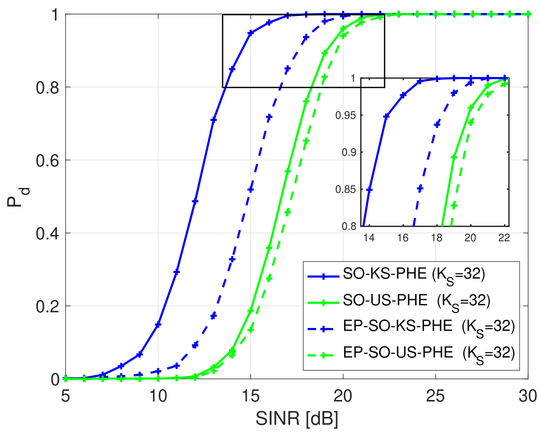

Fig. 13. Second-order detectors for partially-homogeneous environment: $N = 16, K_P = 16, r = 2, K_S = 32$, and $P_{fa} = 10^{-3}$.

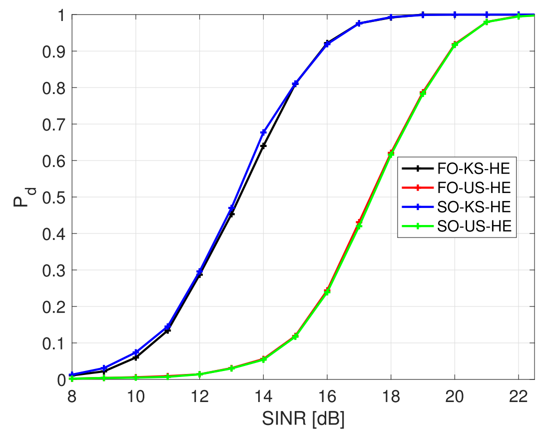

Fig. 15. First-order and second-order detectors for homogeneous environment and the deterministic model of Section III-A for the α_ks: $N = 16, K_P = 32, r = 2, K_S = 24$, and $P_{fa} = 10^{-3}$.

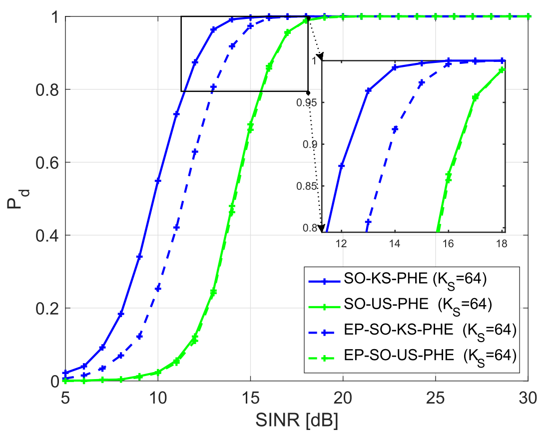

Fig. 14. Second-order detectors for partially-homogeneous environment: $N = 16, K_P = 16, r = 2, K_S = 64$, and $P_{fa} = 10^{-3}$.

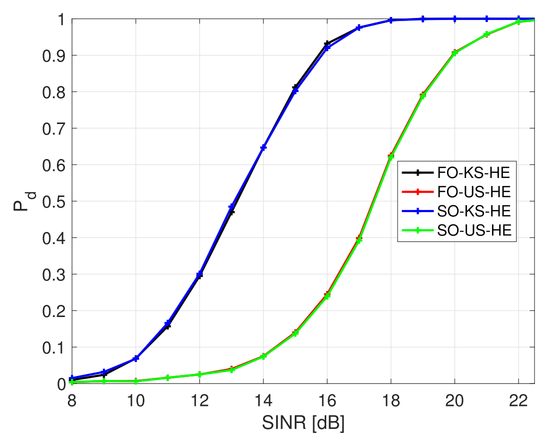

Fig. 16. First-order and second-order detectors for homogeneous environment and the random model of Section III-B for the α_ks: $N = 16, K_P = 32, r = 2, K_S = 24$, and $P_{fa} = 10^{-3}$.

TABLE I
COMPUTATION TIMES [SEC]

			GLR	EP
FO	HE	KS	0.016466	0.007010
		US	0.011722	0.008243
	PHE	KS	0.573772	0.002227
		US	0.427559	0.001512
SO	HE	KS	0.023233	0.013596
		US	0.007919	0.011114
	PHE	KS	0.959086	0.820386
		US	0.364596	0.828431

decision statistics' evaluation excluding the operations required to compute the common terms. The table highlights that the first-order GLR detectors for known subspace detectors are less time-demanding than the second-order counterparts; in the case of unknown subspace, we observe an opposite trend, namely the execution times of the second-order GLR detectors are lower than those of the first-order detectors. Moreover, the EP detectors generally require a lower number of operations than the GLR competitors, except for the EP-SO-US-HE and EP-SO-US-PHE

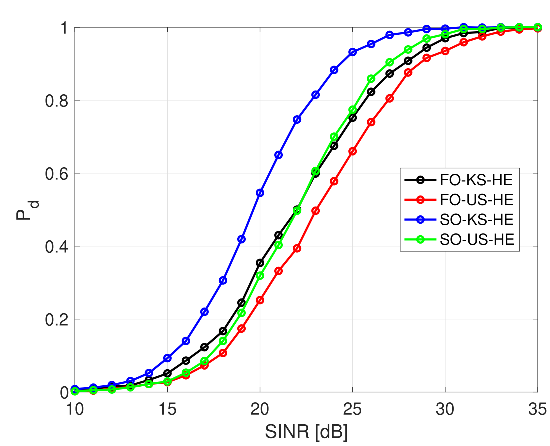

Fig. 17. First-order and second-order detectors for homogeneous environment: $N = 16, K_P = 32, r = 10, K_S = 24$, and $P_{fa} = 10^{-3}$.

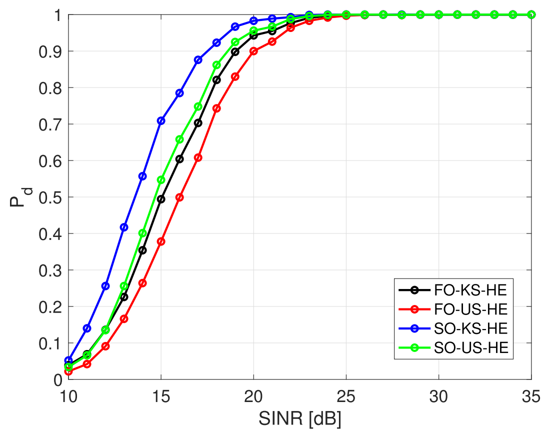

Fig. 18. First-order and second-order detectors for homogeneous environment: $N = 16, K_P = 32, r = 10, K_S = 64$, and $P_{fa} = 10^{-3}$.

that are more time-demanding than their respective counterparts. Finally, notice that the GLR detectors for the partially-homogeneous environment are more time consuming than those for the homogeneous scenario and that the computation times of the GLR detectors for known subspace are greater than those for unknown subspace.

Summarizing, based on the numerical experiments, it appears that the choice of the first-order model versus the second-order model depends in a complicated way on parameter values. Actually, we know no general rule for deciding on one of the proposed approaches. However, when the angular sector becomes wide with a consequent increase of the signal subspace rank, the second-order GLR detectors might be the recommended choice.

IV. Conclusion

In this paper, we have assessed the performance of the GLR detectors derived in the companion paper [1] and compared the performance of these detectors to the performance of EP approximations. It is worth noticing that most of the EP approximations have been derived here for the first time (at least to the best of authors' knowledge). As in [1], we have considered two operating situations: a homogeneous environment where training samples and testing samples share the same statistical characterization of the interference, and a partially-homogeneous environment where training and testing samples differ in scale. The analysis starts by investigating to what extent the P_{fa} is sensitive to variations of the clutter parameters showing that all the GLR detectors maintain a rather constant false alarm rate over the considered parameter ranges. When the signal subspace is known, performance is better than when it is known only by its dimension. The GLR detectors outperform their EP approximants when the signal subspace is known and the number of secondary data is not too large. Finally, the performance of the detectors for an unknown signal subspace are close to each other. Summarizing, the analysis has shown that the design framework proposed in [1] leads to effective solutions for signals with inherent uncertainty that, for a specific radar application, can be related to the angles of arrival, Doppler frequency, and/or phase/amplitude calibration errors.

Future research lines might focus on cases where interference is present. In addition, the analysis on real data and under a mismatch between the actual and the nominal signal subspace represents another research track of interest.

References

[1] D. Orlando, G. Ricci, and L. L. Scharf, "A unified theory of adaptive subspace detection. Part I: Detector designs," *IEEE Trans. Signal Process.*, 2022, doi: 10.1109/TSP.2022.3205761.

[2] F. Bandiera, A. De Maio, A. S. Greco, and G. Ricci, "Adaptive radar detection of distributed targets in homogeneous and partially homogeneous noise plus subspace interference," *IEEE Trans. Signal Process.*, vol. 55, no. 4, pp. 1223–1237, Apr. 2007.

[3] F. Bandiera, O. Besson, D. Orlando, G. Ricci, and L. L. Scharf, "GLRT-based direction detectors in homogeneous noise and subspace interference," *IEEE Trans. Signal Process.*, vol. 55, no. 6, pp. 2386–2394, Jun. 2007.

[4] L. L. Scharf and B. Friedlander, "Matched subspace detectors," *IEEE Trans. Signal Process.*, vol. 42, no. 8, pp. 2146–2157, Aug. 1994.

[5] L. Scharf, S. Kraut, and M. McCloud, "A review of matched and adaptive subspace detectors," in *Proc. IEEE Adaptive Syst. Signal Process. Commun. Control Symp.*, 2000, pp. 82–86.

[6] Y. Hou, W. Zhu, E. Wang, and Y. Zhang, "A hyperspectral subspace target detection method based on AMUSE," *Int. J. Pattern Recognit. Artif. Intell.*, vol. 33, no. 12, 2019, Art. no. 1954032.

[7] N. Acito, M. Moscadelli, M. Diani, and G. Corsini, "Subspace-based target detection in LWIR hyperspectral imaging," *IEEE Geosci. Remote Sens. Lett.*, vol. 17, no. 6, pp. 1047–1051, Jun. 2020.

[8] C.-I. Chang, H. Cao, and M. Song, "Orthogonal subspace projection target detector for hyperspectral anomaly detection," *IEEE J. Sel. Topics Appl. Earth Observ. Remote Sens.*, vol. 14, pp. 4915–4932, 2021.

[9] O. Besson, A. Coluccia, E. Chaumette, G. Ricci, and F. Vincent, "Generalized likelihood ratio test for detection of Gaussian rank-one signals in Gaussian noise with unknown statistics," *IEEE Trans. Signal Process.*, vol. 65, no. 4, pp. 1082–1092, Feb. 2017.

[10] J. Liu, S. Sun, and W. Liu, "One-step persymmetric GLRT for subspace signals," *IEEE Trans. Signal Process.*, vol. 67, no. 14, pp. 3639–3648, Jul. 2019.

[11] J. Liu and J. Li, "Robust detection in MIMO radar with steering vector mismatches," *IEEE Trans. Signal Process.*, vol. 67, no. 20, pp. 5270–5280, Oct. 2019.

[12] E. J. Kelly and K. Forsythe, "Adaptive detection and parameter estimation for multidimensional signal models," Lincoln Lab, MIT, Lexington, MA, USA, Tech. Rep. 848, 1989.

[13] S. Kraut and L. L. Scharf, "The CFAR adaptive subspace detector is a scale-invariant GLRT," *IEEE Trans. Signal Process.*, vol. 47, no. 9, pp. 2538–2541, Sep. 1999.

[14] M. N. Desai and R. S. Mangoubi, "Robust Gaussian and non-Gaussian matched subspace detection," *IEEE Trans. Signal Process.*, vol. 51, no. 12, pp. 3115–3127, Dec. 2003.

[15] F. Gini and A. Farina, "Vector subspace detection in compound-Gaussian clutter. Part I: Survey and new results," *IEEE Trans. Aerosp. Electron. Syst.*, vol. 38, no. 4, pp. 1295–1311, Oct. 2002.

[16] G. Ricci and L. L. Scharf, "Adaptive radar detection of extended Gaussian targets," in *Proc. 12th Annu. Adaptive Sensor Array Process. Workshop*, Lexington, MA, USA, Mar. 16-18, 2004, vol. 1.

[17] F. C. Robey, D. R. Fuhrmann, E. J. Kelly, and R. Nitzberg, "A CFAR adaptive matched filter detector," *IEEE Trans. Aerosp. Electron. Syst.*, vol. 28, no. 1, pp. 208–216, Jan. 1992.

[18] P. Stoica and Y. Selen, "Cyclic minimizers, majorization techniques, and the expectation-maximization algorithm: A refresher," *IEEE Signal Process. Mag.*, vol. 21, no. 1, pp. 112–114, Jan. 2004.

[19] S. Han, L. Yan, Y. Zhang, P. Addabbo, C. Hao, and D. Orlando, "Adaptive radar detection and classification algorithms for multiple coherent signals," *IEEE Trans. Signal Process.*, vol. 69, pp. 560–572, 2021.

[20] J. Ward, "Space-time adaptive processing for airborne radar," MIT Lincoln Lab., Lexington, MA, USA, Tech. Rep. 1015, 1994.

[21] Y. Bresler, "Maximum likelihood estimation of a linearly structured covariance with application to antenna array processing," in *Proc. 4th Annu. ASSP Workshop Spectr. Estimation Model.*, 1988, pp. 172–175.

[22] F. Bandiera, D. Orlando, and G. Ricci, *Advanced Radar Detection Schemes Under Mismatched Signal Models*. San Rafael, CA, USA: Morgan & Claypool Publishers, 2009.
[23] P. Addabbo, S. Han, D. Orlando, and G. Ricci, "Learning strategies for radar clutter classification," *IEEE Trans. Signal Process.*, vol. 69, pp. 1070–1082, 2021.
[24] L. Yan, P. Addabbo, C. Hao, D. Orlando, and A. Farina, "New ECCM techniques against noiselike and/or coherent interferers," *IEEE Trans. Aerosp. Electron. Syst.*, vol. 56, no. 2, pp. 1172–1188, Apr. 2020.
[25] A. Pezeshki, B. D. Van Veen, L. L. Scharf, H. Cox, and M. L. Nordenvaad, "Eigenvalue beamforming using a multirank MVDR beamformer and subspace selection," *IEEE Trans. Signal Process.*, vol. 56, no. 5, pp. 1954–1967, May 2008.
[26] G. Golub and C. V. Loan, *Matrix Computations*. Baltimore, MD, USA: Johns Hopkins Univ. Press, 2013.

Pia Addabbo (Senior Member, IEEE) received the B.Sc. and M.Sc. degrees in telecommunication engineering, and the Ph.D. degree in information engineering from the Universitá degli Studi del Sannio, Benevento, Italy, in 2005, 2008, and 2012, respectively. She is currently an Associate Professor with the Giustino Fortunato University, Benevento, Italy. She is the coauthor of scientific publications in international journals and conferences. Her research interests include statistical signal processing applied to radar target recognition, global navigation satellite system reflectometry, and hyperspectral unmixing. She is currently an Associate Editor for the IEEE TRANSACTIONS ON SIGNAL PROCESSING and IEEE ACCESS.

Danilo Orlando (Senior Member, IEEE) was born in Gagliano del Capo, Italy, on August 9, 1978. He received the Dr. Eng. degree (with Hons.) in computer engineering and the Ph.D. degree (with max. score) in information engineering from the University of Salento (formerly University of Lecce), Lecce, Italy, in 2004 and 2008, respectively. From July 2007 to July 2010, he was with the University of Cassino, Cassino, Italy, engaged in a Research Project on algorithms for track-before-detect of multiple targets in uncertain scenarios. From September to November 2009, he was a Visiting Scientist with the NATO Undersea Research Centre, La Spezia, Italy. From September 2011 to April 2015, he was with Elettronica S.p.A. engaged as System Analyst with the field of electronic warfare. In May 2015, he joined Università degli Studi Niccolò Cusano, Rome, Italy, where he is currently an Associate Professor. In 2007, he has held Visiting Positions with the Department of Avionics and Systems, ENSICA (now Institut Supérieur de l'Aéronautique et de l'Espace, ISAE), Toulouse, France, and from 2017 to 2019, with Chinese Academy of Science, Beijing, China. He is the author or coauthor of more than 150 scientific publications in international journals, conferences, and books. His main research interests include statistical signal processing with more emphasis on adaptive detection and tracking of multiple targets in multisensor scenarios. He was the Senior Area Editor of the IEEE TRANSACTIONS ON SIGNAL PROCESSING and the Associate Editor for the IEEE OPEN JOURNAL ON SIGNAL PROCESSING, *EURASIP Journal on Advances in Signal Processing*, and *MDPI Remote Sensing*.

Giuseppe Ricci (Senior Member, IEEE) was born in Naples, Italy, on February 15, 1964. He received the Dr. and Ph.D. degrees in electronic engineering from the University of Naples "Federico II", Naples, Italy, in 1990 and 1994, respectively. Since 1995, he has been with the University of Salento (formerly University of Lecce), Lecce, Italy, as an Assistant Professor of telecommunications and since 2002, as a Professor. During 1997–1998 and in April/May 2001, he has held Visiting Positions with the University of Colorado, Boulder, CO, USA. In July/September 2003, March 2005, September 2009, and March 2011, respectively, he has held Visiting Positions with Colorado State University, Fort Collins, CO, USA. In March 2006, he has held a Visiting Position with Ensica, Toulouse, France. In September 2008, he has held a Visiting Position with the University of Connecticut, Storrs, CT, USA, and with Arizona State University, Tempe, AZ, USA, in July/August 2019. His research interests are in the field of statistical signal processing with emphasis on radar processing, localization algorithms, and CDMA systems. He is the Member of the Multisensor Target Tracking Working Group, operating under the auspices of the International Society of Information Fusion (ISIF), from 2012 till 2016, and of the Special Area Team *Eurasip Signal Processing for Multisensor Systems* (SPMuS) from 2016 till 2021. He is also the tutorial Co-Chair of the 2020 IEEE Radar Conference, Florence, Italy, 21–25 September, 2020, and the Rector Delegate for teaching activities and continuing education from February 2016 and June 2016, respectively, till April 2017.

Louis L. Scharf (Life Fellow, IEEE) received the Ph.D. degree from University of Washington, Seattle, WA, USA, in 1969. He is currently Research Professor of Mathematics and Emeritus Professor of Electrical and Computer Engineering at Colorado State University, Fort Collins, CO, USA. He holds a courtesy appointment in Statistics. He has coauthored the books, *Statistical Signal Processing: Detection, Estimation, and Time Series Analysis*, Addison-Wesley, 1991, *Statistical Signal Processing of Complex-Valued Data: The Theory of Improper and Noncircular Signals*, Cambridge University Press, 2010. His coauthored book, *A First Course in Electrical and Computer Engineering*, Addison-Wesley, Reading, MA, 1990, was republished by Connexions in 2008. The coauthored book, *Coherence in Signal Processing and Machine Learning*, Springer, will appear in Fall 2022. His research interests include statistical signal processing and machine learning as they apply to space-time adaptive processing for radar, sonar, and communication, modal analysis for electric power system monitoring, spectrum analysis for nonstationary times series modeling, hyperspectral imaging, and image processing for group-invariant classification and registration. Prof. Scharf was the recipient of several awards for his contributions to statistical signal processing, including the Technical Achievement and Society Awards from the IEEE Signal Processing Society, Donald W. Tufts Award for Underwater Acoustic Signal Processing, Diamond Award from the University of Washington, and 2016 IEEE Jack S. Kilby Medal for Signal Processing. In 2021, he received the Education Award from the IEEE Signal Processing Society.